# Identification and Representation of Homotopy Classes of Trajectories for Search-based Path Planning in 3D

Subhrajit Bhattacharya
Department of Mechanical Engineering and Applied Mechanics
University of Pennsylvania
Philadelphia, PA 19104
Email: subhrabh@seas.upenn.edu

Maxim Likhachev
Department of Computer and Information Science
University of Pennsylvania
Philadelphia, PA 19104
Email: maximl@seas.upenn.edu

Vijay Kumar
Department of Mechanical Engineering and Applied Mechanics
University of Pennsylvania
Philadelphia, PA 19104
Email: kumar@seas.upenn.edu

***Abstract*— There are many applications in motion planning where it is important to consider and distinguish between different *homotopy classes* of trajectories. Two trajectories are homotopic if one trajectory can be continuously deformed into another without passing through an obstacle, and a homotopy class is a collection of homotopic trajectories. In this paper we consider the problem of robot exploration and planning in three-dimensional configuration spaces to (a) identify and classify different homotopy classes; and (b) plan trajectories constrained to certain homotopy classes or avoiding specified homotopy classes. In previous work [1] we have solved this problem for two-dimensional, static environments using the Cauchy Integral Theorem in concert with graph search techniques. The robot workspace is mapped to the complex plane and obstacles are poles in this plane. The Residue Theorem allows the use of integration along the path to distinguish between trajectories in different homotopy classes. However, this idea is fundamentally limited to two dimensions. In this work we develop new techniques to solve the same problem, but in three dimensions, using theorems from electromagnetism. The Biot-Savart law lets us design an appropriate vector field, the line integral of which, using the integral form of Ampere's Law, encodes information about homotopy classes in three dimensions. Skeletons of obstacles in the robot world are extracted and are modeled by current-carrying conductors. We describe the development of a practical graph-search based planning tool with theoretical guarantees by combining integration theory with search techniques, and illustrate it with examples in three-dimensional spaces such as two-dimensional, dynamic environments and three-dimensional static environments.** [1]

## I. Introduction

Homotopy classes of trajectories arise due to presence of obstacles in an environment. Two trajectories connecting the same start and goal coordinates are in the same homotopy class if they can be smoothly deformed into one another without intersecting any obstacle in the environment, otherwise they are in different homotopy classes. In many applications, it is important to distinguish between trajectories of different homotopy classes, as well as identify the different homotopy classes in an environment (*e.g.*, trajectories that go left around a circle in two dimensions versus right). For example, in order to deploy a group of agents to explore an environment [4], an efficient strategy ought to be able to identify the multiple homotopy classes and deploy at least one agent in each homotopy class. One may also wish to determine the least cost path for each agent constrained to or avoiding specified homotopy classes. In many problems the notion of *visibility* is linked intrinsically with homotopy classes. In tracking of uncertain agents in an environment with dynamic obstacles, the ability to deal with occlusions during a certain time frame is important [17]. A knowledge of the possible homotopy classes of trajectories that the agent can take in the environment during the period of occlusion can help more efficient belief propagation.

Classification of homotopy classes in two-dimensional workspaces has been studied in robotics literature using geometric methods [7, 10], probabilistic road-map construction [15] techniques and triangulation-based path planning [5]. However, efficient planning for least cost trajectories with homotopy class constraints is not feasible using such representations. In our recent work [1] we have used complex analysis and graph search-based path planning techniques for addressing the problem of optimal path planning with homotopy class constraints. It gave us a compact way of representing homotopy classes of trajectories which is independent of the geometry, discretization of the environment, cost function or search algorithm used to find trajectories in the environment. The method is also robust to noise in the environment created by sensor data. However, this method is only applicable to two dimensional configuration spaces.

In this paper we propose a novel way of classifying and representing homotopy classes in a 3-dimensional configuration space using theorems from electromagnetism. We use Biot-Savart's Law and Ampere's Law to define a differential 1-form [16], the integration of which along trajectories give us an invariant for the homotopy classes of trajectories.

However, there is a technical difference between homology classes of trajectories and their homotopy classes which is

[1]We gratefully acknowledge support from the ONR Antidote MURI project, grant no. N00014-09-1-1031; ONR Grants N00014-08-1-0696 and N00014-09-1-1052; and NSF Grant IIP-0742304.


(a) An unbounded obstacle and its skeleton can be closed at a large distance to create a *closed loop*.

(b) An obstacle with genus 2, $\mathcal{O}$, can be decomposed into 2 obstacles, each with genus one, $\mathcal{O}_1$ and $\mathcal{O}_2$.

Fig. 2. Illustration of Constructions 1 and 2.

worth noting. While in strict mathematical sense, by taking the said integral, the equivalence relation under consideration, and hence the constraints we impose on the planning problems, are *homology* [9, 14] rather than homotopy, we note that in most practical robotics problems the notion of homology and homotopy of trajectories can be equated. A detailed discussion on this is provided in Section VI.

The novelty of the work and the advantage of the integration-based representation we propose lies in the fact that not only it allows us to identify/distinguish trajectories in different homotopy classes, but also lets us compute least-cost paths in 3-dimensional configuration spaces with homotopic constraints using graph search-based planning algorithms. The representation we propose is designed to be independent of the type of the environment, the discretization scheme or cost function. Using such a representation we show that homotopy class constraints can be seamlessly integrated with graph search techniques for determining optimal paths constrained to specified homotopy classes or forbidden from others. We also discuss how one can explore multiple homotopy classes in an environment using a single graph search.

## II. Background

### A. Homotopy Classes in Three Dimensional Spaces

While in the two-dimensional case, theoretically any finite obstacle on the plane can induce multiple homotopy classes for trajectories joining two points, the notion of homotopy classes in three dimensions can only be induced by obstacles with *genus* one or more, or with obstacles stretching to infinity in two directions (The *genus* of an obstacle refers to the number of *holes* or *handles* [13]. See Figure 1). For example, a torus-shaped obstacle in a three-dimensional environment creates two primary homotopy classes: *i.* The trajectories passing through the "hole" of the torus, and *ii.* the trajectories passing outside the "hole" of the torus. Figure 1 shows some examples of obstacles that can or cannot induce homotopy classes for trajectories. A sphere or a solid cube, for example, cannot induce multiple homotopy classes in an environment.

**Definition 1 (Simple Homotopy-Inducing Obstacle):** A *Simple Homotopy-inducing Obstacle* (SHIO) is a bounded obstacle of *genus* 1, for example a torus (Figure 1(a), 1(b)) or a knot (Figure 1(e)).

### B. Skeleton *of a SHIO*

In [1], each obstacle in a 2-dimensional plane that induces the notion of multiple homotopy classes is assigned a *representative point*. Analogously, for the 3-dimensional case, we need to define a *skeleton* for every SHIO. Intuitively, a skeleton of a 3-dimensional obstacle is a 1-dimensional curve that is completely contained inside the obstacle such that the surface of the obstacle can be "shrunk" onto the skeleton in a continuous fashion without altering the topology of the surface of the obstacle. Formally, we define the skeleton of an obstacle in terms of *homotopy equivalence*.

**Definition 2 (Skeleton):** A 1-dimensional manifold, $S$, is called a *skeleton* of a SHIO, $\mathcal{O}$, iff $S$ is homeomorphic to $\mathbb{S}^1$ (a circle), $S$ is completely contained inside $\mathcal{O}$, and if $S$ and $\mathcal{O}$ are *homotopy equivalent* (*i.e.*, if the obstacle $\mathcal{O}$ is replaced by an equivalent obstacle $S$, then the *homotopy equivalence* between two arbitrary trajectories, $\tau_1$ and $\tau_2$, connecting every pair of fixed points in the environment, will remain unchanged.)

In the literature, algorithms for constructing skeletons of solid objects is a well-studied [3, 11]. However in the present context we have a much relaxed notion of skeleton. While we can adopt any of the different existing algorithms for automated construction of skeleton from a 3-dimensional obstacles, this discussion is out of the scope of the present work. Figure 1(a) demonstrates how a skeleton can be constructed for a generic genus 1 obstacle. There is definitely no unique way of constructing such a skeleton. For the results in this paper with the $X-Y-Z$ domain, we either hand-picked key-points inside obstacles to construct skeletons, or created obstacles around a *skeleton* to begin with. For the $X-Y-Time$ domain we used similar notion as *representative points* [1] inside moving obstacles, that automatically creates a skeleton for that obstacles in $X-Y-Time$ domain because of extrusion along the time axis.

### C. Conversion of generic obstacles into SHIOs

Given a set of obstacles in a three-dimensional environment, we perform the following two constructions/reduction on the obstacles so that the only kind of obstacle we have in the environment are *Simple Homotopy-Inducing Obstacles*. The Construction 1 is mostly trivial in the sense that it can be easily automated for arbitrary obstacles. Construction 2 on the other hand is linked with the construction of *skeleton* of the obstacles (Definition 2) and is discussed later.

***Construction* 1 (Closing infinite, unbounded obstacles):** In most of the problems that we are concerned with, the domain in which the trajectories of the robots lie is finite and bounded. This gives us the freedom of altering/modifying the obstacles or parts of obstacles lying outside that domain without altering the problem. One consequence of this freedom is that we can *close* infinite and unbounded obstacles (*e.g.* Figure 1(d)) at a large distance from the domain of interest (Figure 2(a)).

***Construction* 2 (Decomposing obstacles with genus $> 1$):** After closing all infinite, unbounded obstacles in an environment according to Construction 1, if there is an obstacle with genus $k$ (*e.g.* Figure 1(c)), we can decomposed/split it into $k$ obstacles, possibly overlapping and touching each other, but each with genus 1 (Figure 2(b)). This does not change the obstacles or the problem in any

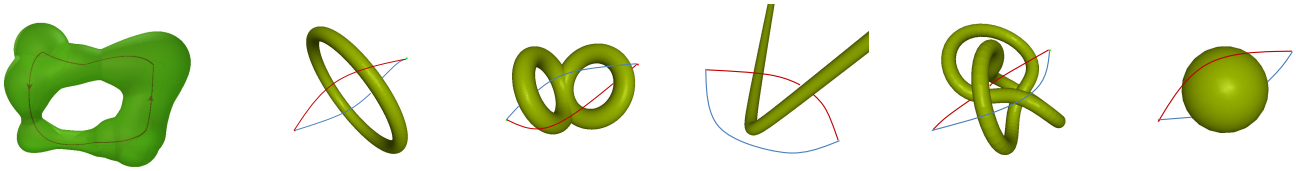

(a) Skeleton of a generic genus 1 obstacle is modeled as a current-carrying conductor.

(b) A torus-shaped genus 1 obstacle.

(c) A genus 2 obstacle.

(d) An infinite tube is a genus 1 obstacle.

(e) A knot-shaped obstacle with genus 1.

(f) A sphere **does not** induce homotopy classes and has genus 0.

Fig. 1. Obstacles that do and do not induce homotopy classes in a 3-dimensional space.

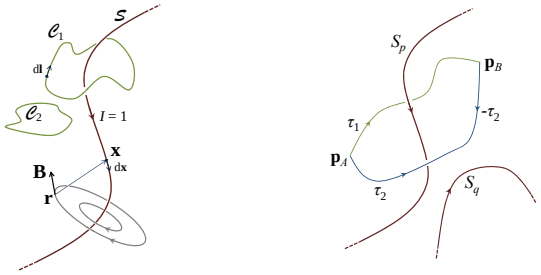


(a) Magnetic field due to current in $\mathcal{S}$, & its integration along closed loop $\mathcal{C}_i$.

(b) 2 trajectories, $\tau_1$ & $\tau_2$, connecting the same points form a closed loop.

Fig. 3.

way. This construction just changes the way we identify obstacles. For example in Figure 2(b) the original obstacle $\mathcal{O}$ with genus 2 is realized as two obstacles $\mathcal{O}_1$ and $\mathcal{O}_2$, each with genus 1 and overlapping each other. The decomposition of obstacles into SHIOs allows us define $k$ skeletons for each obstacle of genus $k$ and simplify computations of *h*-signatures of trajectories.

### D. Biot-Savart law

Consider a single hypothetical current-carrying *curve* (a current conducting wire) embedded in a 3-dimensional space carrying a steady current of unit magnitude (Figure 3(a)). It is to be noted that such a steady current is possible iff the *curve* is closed (or open, but extending to infinity, where we close the curve using a loop at infinity. See Figure 2(a) and Construction 1). We denote the curve by $\mathcal{S}$. Then, according to the Biot-Savart Law [6], the magnetic field $\mathbf{B}$ at any arbitrary point $\mathbf{r}$ in the space, due to the current flow in $\mathcal{S}$, is given by,

$$\mathbf{B}(\mathbf{r}) = \frac{\mu_0}{4\pi} \int_{\mathcal{S}} \frac{(\mathbf{x} - \mathbf{r}) \times \mathrm{d}\mathbf{x}}{\|\mathbf{x} - \mathbf{r}\|^3} \tag{1}$$

where, $\mathbf{x}$, the integration variable, represents the coordinate of a point on $\mathcal{S}$, and $d\mathbf{x}$ is an infinitesimal element on $\mathcal{S}$ along the direction of the current flow.

### E. Ampere's Law

While Biot-Savart law gives a recipe for computing the magnetic field from a given current configuration, Ampere's Law [6], in a sense, gives the inverse of it. Given the magnetic field $\mathbf{B}$ at every point in the space, and a closed loop $\mathcal{C}$ (Figure 3(a)), the line integral of $\mathbf{B}$ along $\mathcal{C}$ gives the current *enclosed* by the loop $\mathcal{C}$. That is,

$$\Xi(\mathcal{C}) := \int_{\mathcal{C}} \mathbf{B}(\mathbf{l}) \cdot \mathrm{d}\mathbf{l} = \mu_0 I_{encl} \tag{2}$$

where, $\mathbf{l}$, the integration variable, represents the coordinate of a point on $\mathcal{C}$, and $d\mathbf{l}$ is an infinitesimal element on $\mathcal{C}$.

In Biot-Savart Law and Ampere's Law one can conveniently choose the constant $\mu_0$ to be equal to 1 by proper choice of units. Moreover, by choice, the value of the current flowing in the conductor is unity. Thus, for any closed loop $\mathcal{C}$, the value of $\Xi(\mathcal{C})$ is zero iff $\mathcal{C}$ does not enclose the conductor, otherwise it is $\pm 1$ (the sign depends on the direction of integration performed on $\mathcal{C}$). Thus in Figure 3(a), $\Xi(\mathcal{C}_1) = 1$ and $\Xi(\mathcal{C}_2) = 0$.

## III. Application of Theory of Electromagnetism in Identifying Homotopy Classes

### A. Skeleton of SHIOs as Current Carrying Manifolds

***Construction* 3: (Modeling *skeleton* of a SHIO as a current carrying manifold)** This is the key construction: Given $m$ obstacles in an environment, $\mathcal{O}_1, \mathcal{O}_2, \ldots, \mathcal{O}_m$, with genus $k_1, k_2, \ldots, k_m$ respectively, we can construct $M = k_1 + k_2 + \cdots + k_m$ skeletons from $M$ SHIOs (obtained using Constructions 1 and 2), namely $S_1, S_2, \ldots, S_M$. Each $S_i$ is a closed, connected, boundary-less 1-dimensional manifold. We model each of them as a current-carrying conductor carrying current of unit magnitude (Figures 1(a), 2(a)). The direction of the currents is not of importance, but by convention, each is of unit magnitude.

**Definition 3 (Virtual Magnetic Field due to a Skeleton):** Given $S_i$, the skeletons of a Simple Homotopy-Inducing Obstacle, we define a *Virtual Magnetic Field vector* at a point $\mathbf{r}$ in the space due to the current in $S_i$ using Ampere's Law as follows,

$$\mathbf{B}_i(\mathbf{r}) = \frac{1}{4\pi} \int_{S_i} \frac{(\mathbf{x} - \mathbf{r}) \times \mathrm{d}\mathbf{x}}{\|\mathbf{x} - \mathbf{r}\|^3} \tag{3}$$

where, $\mathbf{x}$, the integration variable, represents the coordinates of a point on $S_i$, and $d\mathbf{x}$ is an infinitesimal element on $S_i$ along the chosen direction of the current flow in $S_i$.

### B. h-Signature

**Definition 4 (*h*-Signature):** Given an arbitrary trajectory, $\tau$, in the 3-dimensional environment with $M$ skeletons, we define the *h-signature* of $\tau$ to be the following $M$-vector,

$$\mathcal{H}(\tau) = [h_1(\tau),\ h_2(\tau),\ \ldots,\ h_M(\tau)]^T \tag{4}$$

where,

$$h_i(\tau) = \int_{\tau} \mathbf{B}_i(\mathbf{l}) \cdot \mathrm{d}\mathbf{l} \tag{5}$$

is defined in an analogous manner as the integral in Ampere's Law. In defining $h_i$, $\mathbf{B}_i$ is the *Virtual Magnetic Field* vector due to the unit current through skeleton $S_i$, $\mathbf{l}$ is the integration variable that represents the coordinate of a point on $\tau$, and $d\mathbf{l}$ is an infinitesimal element on $\tau$.

**Lemma 1:** If two trajectories $\tau_1$ and $\tau_2$ connecting the same pair of fixed end points belong to the same homotopy class, then their *h*-signatures are the same.

*Sketch of Proof:* Since $\tau_1$ and $\tau_2$ connect the same points, $\tau_1 \cup -\tau_2$, *i.e.* $\tau_1$ and $-\tau_2$ together (where $-\tau$ indicates the same curve as $\tau$, but with the opposite orientation) form a closed loop in the 3-dimensional environment (Figure 3(b)). We replace the obstacles $\mathcal{O}_1, \mathcal{O}_2, \ldots, \mathcal{O}_m$ in the environments with the skeletons $S_1, S_2, \ldots, S_M$.

Consider the presence of just the skeleton $S_i$. By the direct consequence of Ampere's Law and our construction in which a unit current flows through $S_i$, the value of

$$h_i(\tau_1 \cup -\tau_2) = \int_{\tau_1 \cup -\tau_2} \mathbf{B}_i(\mathbf{l}) \cdot \mathrm{d}\mathbf{l}$$

is non-zero if the closed loop formed by $\tau_1 \cup -\tau_2$ encloses the current carrying conductor $S_i$. Otherwise it is zero. For example, in Figure 3(b), $h_p(\tau_1 \cup -\tau_2) = 1$ and $h_q(\tau_1 \cup -\tau_2) = 0$. A direct consequence of this fact is that $h_i(\tau_1 \cup -\tau_2) = 0$ if $\tau_1$ can be smoothly deformed into $\tau_2$ without intersecting $S_i$. Now, by the definition of line integration we have the following identity,

$$\begin{aligned} h_i(\tau_1 \cup -\tau_2) &= \textstyle\int_{\tau_1 \cup -\tau_2} \mathbf{B}_i(\mathbf{l}) \cdot \mathrm{d}\mathbf{l} \\ = \textstyle\int_{\tau_1} \mathbf{B}_i(\mathbf{l}) \cdot d\mathbf{l} - \int_{\tau_2} \mathbf{B}_i(\mathbf{l}) \cdot \mathrm{d}\mathbf{l} &= h_i(\tau_1) - h_i(\tau_2) \end{aligned} \tag{6}$$

Thus, $h_i(\tau_1) = h_i(\tau_2)$ if $\tau_1$ can be smoothly deformed into $\tau_2$ without intersecting $S_i$ (*i.e* homotopic).

Now in presence of skeletons $S_1, S_2, \ldots, S_M$ the same argument extends for each skeleton individually. Thus $\tau_1$ and $\tau_2$ being homotopic will imply that their *h*-signatures are the same. ■

**Assumption 1:** The converse statement of Lemma 1 holds true in most practical robotics problems and applications.

*Reasoning:* The converse statement of Lemma 1 would read *"Two trajectories $\tau_1$ and $\tau_2$ connecting the same pair of fixed end points belong to the same homotopy class if their h-signatures are the same."*. While this statement at the first glance appears quite intuitive using the same logic as before, it in fact does not hold true in an universal sense.

The reason, as discussed earlier, is that the *h*-signature we formulate is in fact a *homology invariant* rather than a *homotopy invariant* of trajectories. Thus, if in the above statement, we replace "homotopy" with "homology", the statement becomes a *lemma*. As we will discuss in greater details in Section VI, the notion of homology, though more abstract than homotopy, was developed as a part of *algebraic topology* because of the fact that homotopy is difficult computationally. While homology serves as a fair analog for homotopy in many respects, there are subtle differences between two.

However, in robotics applications, for most practical scenarios, this separation is little. For example, homotopy and homology classes of trajectories are one and the same for trajectories in 3-dimensional configuration spaces with unbounded obstacles (*e.g.* $X - Y - Time$ configuration space). In such environments Assumption 1 becomes a lemma. Moreover, out of the two types of problems we will consider, the one in which we explore/find least cost trajectories in different homotopy classes in an environment, we are guaranteed to find trajectories in distict homotopy classes without even the need of Assumption 1 being true. This is because homotopic trajectories are always guaranteed to be homologous [9].

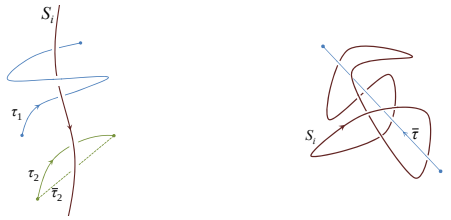


(a) Trajectory that loops around a skeleton & one that doesn't. In this figure $h_i(\tau_1) > 1$ and $0 < h_i(\tau_2) = h_i(\overline{\tau}_2) < 1$.

(b) In the most general case, it is difficult to precisely identify a *non-looping* homotopy class.

Fig. 4.

In Section VI we discuss this in greater details and its implications in robot planning problems. ■

### C. Some notes on the value of h-Signature

"Looping" of a trajectory around an obstacle (Figure 4(a)) is similar in essence to *non-Jordan* curves on two-dimensional planes. However in three dimensions their precise and universal definition is more difficult. One way of identifying one of the homotopy classes of trajectories (joining a given start and an end coordinate) that do not loop around a skeleton $S_i$ is by joining the start and the end coordinates using a straight line segment (call it $\overline{\tau}$). Then the trajectories that are homotopic to $\overline{\tau}$ form a particular homotopy class of *non-looping trajectories* w.r.t. $S_i$ (for example, in Figure 4(a), the homotopy class to which $\overline{\tau}_2$, and hence $\tau_2$, belong are non-looping). However, for more complex obstacles (like knots), the notion of a *non-looping* trajectory being a straight line segment breaks down (See Figure 4(b)). In fact the notions of *looping* and *non-looping* is imprecise in such cases. In [2] we show that for the special simple case when $S_i$ is an infinitely long line, the component of the *h*-signature $h_i(\overline{\tau})$ for a line segment $\overline{\tau}$ lies between $-1$ and 1. We hence propose the following mathematical definition of a *non-looping* trajectory,

**Definition 5 (Non-looping trajectory w.r.t. $S_i$):** A trajectory $\tau$ is said to be *non-looping* w.r.t. $S_i$ if $h_i(\tau) \in (-1, 1)$. The value is in $[0, 1)$ if the trajectory goes around $S_i$ in accordance with the *right-hand rule* with thumb pointing along the direction of the current in $S_i$. If the direction is opposite, the value lies in $(-1, 0]$.

This definition, in many cases, conform to our general intuition of *non-looping* trajectories. If another trajectory, $\tau'$, connecting the same start and end points as a non-looping trajectory $\tau$, goes on the "other side of the obstacle" without looping around it, then $\tau \cup -\tau'$ forms a closed loop that encloses $S_i$. Then, $h_i(\tau \cup -\tau') = \pm 1 = \text{sign}(h_i(\tau \cup -\tau'))$. But since, $\tau$ and $\tau \cup -\tau'$ goes around $S_i$ in the same orientation, we have $\text{sign}(h_i(\tau \cup -\tau')) = \text{sign}(h_i(\tau))$. Again by property of line integration, $h_i(\tau \cup -\tau') = h_i(\tau) - h_i(\tau')$. Thus, $h_i(\tau') = h_i(\tau) - \text{sign}(h_i(\tau))$. Thus we have the following definition.

**Definition 6 (Complementary Homotopy Class):** Given a trajectory $\tau$ that is *non-looping* w.r.t. all the skeletons in the environment (*i.e.* $h_i(\tau) \in (-1, 1)\ \forall\ i = 1, 2, \ldots, M$), we define the *Complementary Homotopy Class* of the

homotopy class of $\tau$ to be the one for which the *h*-signature is $\mathcal{H}(\tau) - \text{sign}(\mathcal{H}(\tau))$, where sign$(\cdot)$ gives the vector of signs of the elements of its input vector.

## IV. Search-based Planning in Three Dimensions with Homotopy Class Constraints

We now investigate the problem of search-based path planning for trajectories in 3-dimensional configuration spaces. Primarily we investigate two types of problems: (i.) Exploration of the different homotopy classes of trajectories connecting a given start and goal coordinates in the environment, and (ii.) Planning for trajectories with specified homotopy class constraints (where we are required to find trajectories restricted to specified homotopy classes, and/or avoiding other specified homotopy classes). We perform these tasks in two kinds of environments: *a)* two-dimensional dynamic environment, and *b)* three-dimensional static environment.

In the discussion that follows, we represent a point in the 3-dimensional configuration space using the coordinates $\mathbf{v} = (x, y, z)$, with the understanding that $z$ can represent $time$ in the time-varying 2-dimensional environment.

The approach, as in [1], is to discretize the configuration space, construct a directed graph out of it, and perform a graph search in it. The discretization can be quite general. Approximate or exact cell decompositions can be used to generate a roadmap. The roadmap can be probabilistic or deterministic. Or a uniform grid representation can be used to generate a graph, which is the representation used here. The discretized space is represented by the graph $\mathcal{G} = (\mathcal{V}, \mathcal{E})$, in which each node $\mathbf{v} = (x, y, z) \in \mathcal{V}$ represents the coordinate of a discretized cell. Depending on the type of configuration space, the nodes are connected to their relevant neighboring nodes by weighted edges, where the weights are equal to the cost of traversing the edge. A directed edge connecting node $\mathbf{v}_1$ to $\mathbf{v}_2$ is represented by $\{\mathbf{v}_1 \rightarrow \mathbf{v}_2\}$. Inaccessible coordinates (lying inside obstacles or outside a specified workspace) do not constitute nodes of the graph. A path in this graph represents a trajectory of the robot in the 3-dimensional configuration space. Moreover, small obstacles (*e.g.* created by sensor noise), or obstacles that we don't desire to contribute towards the homotopy class of trajectories, can be chosen not to have a skeleton, thus preventing them from claiming a component in the *h*-signature vector.

We will discuss the connectivity of the graph, $\mathcal{G}$, and the cost function in greater details for each of the two types of configuration space we present in Section V.

### A. Computation of h-Signature for an Edge of $\mathcal{G}$

For all practical applications we assume that a skeleton of an obstacle, $S_i$, is made up of finite number ($n_i$) of line segments: $S_i = \{\overrightarrow{\mathbf{s}_i^1\mathbf{s}_i^2},\ \overrightarrow{\mathbf{s}_i^2\mathbf{s}_i^3},\ \ldots,\ \overrightarrow{\mathbf{s}_i^{n_i-1}\mathbf{s}_i^{n_i}},\ \overrightarrow{\mathbf{s}_i^{n_i}\mathbf{s}_i^1}\}$ (Figure 5(a)). Thus, the integration of equation (3) can be split into summation of $n_i$ integrations,

$$\mathbf{B}_i(\mathbf{r}) = \frac{1}{4\pi}\sum_{j=1}^{n_i}\int_{\overrightarrow{\mathbf{s}_i^j\mathbf{s}_i^{j'}}} \frac{(\mathbf{x}-\mathbf{r})\times \mathrm{d}\mathbf{x}}{\|\mathbf{x}-\mathbf{r}\|^3} \tag{7}$$

where $j' \equiv 1 + (j \mod n_i)$.

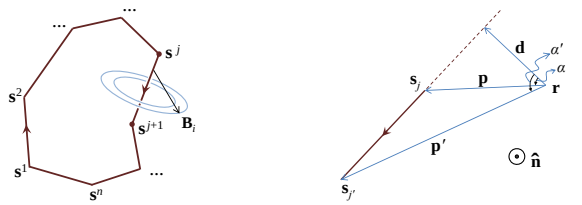


(a) A skeleton of an obstacle can be constructed/approximated so that it is made up of $n$ line segments.

(b) Magnetic field at $\mathbf{r}$ due to the current in a line segment $\overrightarrow{\mathbf{s}_i^j\mathbf{s}_i^{j'}}$.

Fig. 5.

One advantage of this representation of skeletons is that for the straight line segments, $\overrightarrow{\mathbf{s}_i^j\mathbf{s}_i^{j'}}$, the integration can be computed analytically. Specifically, using a result from [6] (also, see Figure 5(b)),

$$\begin{aligned}\int_{\overrightarrow{\mathbf{s}_i^j\mathbf{s}_i^{j'}}} \frac{(\mathbf{x}-\mathbf{r})\times \mathrm{d}\mathbf{x}}{\|\mathbf{x}-\mathbf{r}\|^3} &= \frac{1}{\|\mathbf{d}\|}\left(\sin(\alpha') - \sin(\alpha)\right)\hat{\mathbf{n}} \\ &= \frac{1}{\|\mathbf{d}\|^2}\left(\frac{\mathbf{d}\times\mathbf{p}'}{\|\mathbf{p}'\|} - \frac{\mathbf{d}\times\mathbf{p}}{\|\mathbf{p}\|}\right) \end{aligned} \tag{8}$$

where, $\mathbf{d}, \mathbf{p}$ and $\mathbf{p}'$ are functions of $\mathbf{s}_i^j, \mathbf{s}_i^{j'}$ and $\mathbf{r}$ (Figure 5(b)), and can be expressed as,

$$\mathbf{p} = \mathbf{s}_i^j - \mathbf{r},\quad \mathbf{p}' = \mathbf{s}_i^{j'} - \mathbf{r},\quad \mathbf{d} = \frac{(\mathbf{s}_i^{j'} - \mathbf{s}_i^j)\times(\mathbf{p}\times\mathbf{p}')}{\|\mathbf{s}_i^{j'} - \mathbf{s}_i^j\|^2} \tag{9}$$

We define and write $\mathbf{\Phi}(\mathbf{s}_i^j, \mathbf{s}_i^{j'}, \mathbf{r})$ for the RHS of Equation (8) for notational convenience. Thus we have,

$$\mathbf{B}_i(\mathbf{r}) = \frac{1}{4\pi}\sum_{j=1}^{n_i} \mathbf{\Phi}(\mathbf{s}_i^j, \mathbf{s}_i^{j'}, \mathbf{r}) \tag{10}$$

where, $j' \equiv 1 + (j \mod n_i)$.

Given an edge $e \in \mathcal{E}$, we can now compute the *h-signature*, $\mathcal{H}(e) = [h_1(e),\ h_2(e),\ \ldots,\ h_M(e)]^T$, where,

$$h_i(e) = \frac{1}{4\pi}\int_e \sum_{j=1}^{n_i} \mathbf{\Phi}(\mathbf{s}_i^j, \mathbf{s}_i^{j'}, \mathbf{l})\cdot \mathrm{d}\mathbf{l} \tag{11}$$

can be computed numerically.

### B. h-Signature Augmented Graph

Let $\mathbf{v}_s = (x_s, y_s, z_s)$ be the start coordinate in the configuration space, and $\mathbf{v}_g = (x_g, y_g, z_g)$ be the goal coordinate. By Lemma 1 and Assumption 1, any two trajectories from $\mathbf{v}_s$ to $\mathbf{v}$ that belong to the same homotopy class will have the same *h*-signature. The *h*-signature can assume different, but discrete values corresponding on the homotopy class of the trajectory. We also write $\mathcal{P}(\mathbf{v}_s, \mathbf{v})$ to denote the set of all trajectories from $\mathbf{v}_s$ to $\mathbf{v}$, and $\widetilde{\mathbf{v}_s\mathbf{v}} \in \mathcal{P}(\mathbf{v}_s, \mathbf{v})$ to denote a particular trajectory in that set.

*1) Allowed and Blocked Homotopy Classes:* Suppose it is required that we restrict all our search for trajectories connecting $\mathbf{v}_s$ and $\mathbf{v}_g$ to certain homotopy classes, or not allow certain homotopy classes. We denote the set of allowed *h*-signatures of trajectories leading up to $\mathbf{v}_g$ by the set $\mathcal{A}$, and the set of blocked *h*-signatures as $\mathcal{B}$. $\mathcal{A}$ and $\mathcal{B}$ are essentially complement of each other ($\mathcal{A} \cup \mathcal{B} = \mathcal{U}$, where the universal set, $\mathcal{U}$, is the set of the *h*-signatures of all the homotopy classes of trajectories joining $\mathbf{v}_s$ and $\mathbf{v}_g$), and $\mathcal{B}$ can be an empty set when all homotopy classes are allowed. Following

the discussion in Section III-C, it is also possible to restrict search to *non-looping* trajectories by putting all *h*-signatures that have at least one element outside $(-1, 1)$ into the set $\mathcal{B}$.

*2) h-Signature Augmented Graph:* Once we have the means of computing *h*-signature for each edge, we introduce the concept of *h-signature augmented graph*. We define the *h-signature augmented graph* of $\mathcal{G}$ as the graph $\mathcal{G}_H(\mathcal{G}) = \{\mathcal{V}_H, \mathcal{E}_H\}$, such that each node in this new graph has the *h*-signature of a trajectory leading up to the coordinate of the node from $\mathbf{v}_s$ appended to it. That is, each node in this augmented graph is given by $\{\mathbf{v}, \mathcal{H}(\widetilde{\mathbf{v}_s\mathbf{v}})\}$, for some $\widetilde{\mathbf{v}_s\mathbf{v}} \in \mathcal{P}(\mathbf{v}_s, \mathbf{v})$. Thus, corresponding to a given $\mathbf{v} \in \mathcal{V}$, since there are discrete homotopy classes of trajectories from $\mathbf{v}_s$ to $\mathbf{v}$, there are a discrete number of the augmented states, $\{\mathbf{v}, \mathbf{h}\} \in \mathcal{V}_H$, where $\mathbf{h}$ is a $M$-vector and assumes the values of the *h*-signatures corresponding to the discrete homotopy classes. Thus, we define the *h-signature augmented graph* of $\mathcal{G}$ as follows,

$$\mathcal{G}_H = \{\mathcal{V}_H, \mathcal{E}_H\}$$

where,

1. $$\mathcal{V}_H = \left\{ \{\mathbf{v}, \mathbf{h}\} \;\middle|\; \begin{array}{l} \mathbf{v} \in \mathcal{V}, \text{ and,} \\ \mathbf{h} = \mathcal{H}(\widetilde{\mathbf{v}_s\mathbf{v}}) \text{ for some trajectory} \\ \qquad \widetilde{\mathbf{v}_s\mathbf{v}} \in \mathcal{P}(\mathbf{v}_s, \mathbf{v}), \text{ and,} \\ \mathbf{h} \in \mathcal{A} \text{ (equivalently, } \mathbf{h} \notin \mathcal{B}) \\ \qquad \text{when } \mathbf{v} = \mathbf{v}_g \end{array} \right\}$$

2. An edge $\{\{\mathbf{v}, \mathbf{h}\} \to \{\mathbf{v}', \mathbf{h}'\}\}$ is in $\mathcal{E}_H$ for $\{\mathbf{v}, \mathbf{h}\} \in \mathcal{V}_H$ and $\{\mathbf{v}', \mathbf{h}'\} \in \mathcal{V}_H$, iff
   i. The edge $\{\mathbf{v} \to \mathbf{v}'\} \in \mathcal{E}$, and,
   ii. $\mathbf{h}' = \mathbf{h} + \mathcal{H}(\mathbf{v} \to \mathbf{v}')$, where, $\mathcal{H}(\mathbf{v} \to \mathbf{v}')$ is the *h-signature* of the edge $\{\mathbf{v} \to \mathbf{v}'\} \in \mathcal{E}$.
3. The cost/weight associated with an edge $\{\{\mathbf{v}, \mathbf{h}\} \to \{\mathbf{v}', \mathbf{h}'\}\}$ is same as that associated with edge $\{\mathbf{v} \to \mathbf{v}'\} \in \mathcal{E}$.

The consequence of point 3 in the above definition is that an *admissible heuristics* for search in $\mathcal{G}$ will remain admissible in $\mathcal{G}_H$. That is, if $f(\mathbf{v}, \mathbf{v}_g)$ was the heuristic function in $\mathcal{G}$, we define $f_H(\{\mathbf{v}, \mathbf{h}\}, \{\mathbf{v}_g, \mathbf{h}'\}) = f(\mathbf{v}, \mathbf{v}_g)$ as the heuristic function in $\mathcal{G}_H$ for any $\mathbf{h}' \in \mathcal{A}$.

The consequence of augmenting each node of $\mathcal{G}$ with a *h*-signature is that now nodes are distinguished not only by their coordinates, but also the *h*-signature of the trajectory followed to reach it. Typically we use graph search algorithms like A* (or variants like D* or D*-lite) where nodes in the graph $\mathcal{G}_H$ are expanded starting from the node $\{\mathbf{z}_s, \mathbf{0}\}$ (where by $\mathbf{0}$ we mean a $M$-dimensional vector of zeros). For exploration of homotopy classes, whenever we expand a state $\{\mathbf{z}_g, \tilde{\mathbf{h}}\} \in \mathcal{V}_H$, for some $\tilde{\mathbf{h}} \notin \mathcal{B}$, we store the path up to that node, and continue expanding more states until the desired number of homotopy classes are explored. That way we explore homotopy classes in order of their path costs. For searches with homotopy class constraint, we stop upon expansion of a goal coordinate $\{\mathbf{z}_g, \tilde{\mathbf{h}}\}$ for some $\tilde{\mathbf{h}} \notin \mathcal{B}$ (or equivalently, $\tilde{\mathbf{h}} \in \mathcal{A}$).

### C. Theoretical Analysis

**Theorem 1:** If $\mathbf{P}^*_H = \{\{\mathbf{v}_1, \mathbf{h}_1\}, \{\mathbf{v}_2, \mathbf{h}_2\}, \cdots, \{\mathbf{v}_p, \mathbf{h}_p\}\}$ is an optimal path in $\mathcal{G}_H$, then the path $\mathbf{P}^* = \{\mathbf{v}_1, \mathbf{v}_2, \cdots, \mathbf{v}_p\}$ is an optimal path in the graph $\mathcal{G}$ satisfying the *h*-signature constraints specified by $\mathcal{A}$ and $\mathcal{B}$

*Proof:* By construction of $\mathcal{G}_H$, the path $\{\mathbf{v}_1, \mathbf{v}_2, \cdots, \mathbf{v}_p\}$ satisfies the given *h*-signature constraints. Moreover by definition, $\mathbf{P}^*_H$ is a minimum cost path in $\mathcal{G}_H$. Since the cost function in $\mathcal{G}_H$ is the same as the one in $\mathcal{G}$ and does not involve $\mathbf{h}_j$, it follows that the projection of $\mathbf{P}^*_H$ on $\mathcal{G}$ given by $\mathbf{P}^* = \{\mathbf{v}_1, \mathbf{v}_2, \cdots, \mathbf{v}_p\}$ is an optimal path in the graph $\mathcal{G}$ satisfying the constraints defined in $\mathcal{G}_H$. ■

## V. Results

We implemented the graph structure, $\mathcal{G}_H$, and A* search algorithm [8] to search in the graph using C++ programing language. For the numerical integration in Equation (11) we used the GNU Scientific Library. For the graphic visualization we used *OpenCV* and *OpenGL* libraries.

### A. Planning in 3-dimensional space with static obstacles

The first domain in which we implement the planning algorithm is the space of 3 spatial dimensions, $X, Y$ and $Z$. For a particular problem, the domain of interest is bounded by upper and lower limits of the 3 coordinates. The domain is then uniformly discretized into cubic cells and a node of $\mathcal{G}$ is placed at the center of each cell. Connectivity is established between a node and its 26 neighbors (all cells that share at least one corner, edge or face with it). Each edge is bi-directional and its cost is the Euclidean length.

*1) Simple environments with bounded obstacles:* Figure 6(a) demonstrates a simple environment, $20 \times 20 \times 18$ discretized, with two *torus-shaped* obstacles. The skeleton of each obstacle is made up of line segments passing through the central axis of the cylindrical segments. Here we restrict search to *non-looping* trajectories. That is, we set $\mathcal{B} = \left\{\mathbf{h} = [h_1, h_2]^T \;\middle|\; |h_1| > 1 \text{ or } |h_2| > 1\right\}$. We search for 4 homotopy classes of trajectories connecting a given start and goal coordinate. As shown in Figure 6(a), the algorithm finds four such trajectories: (i) going through hoops 1 and 2; (ii) going through hoop 1 but not through hoop 2; (iii) going through hoop 2 but not through hoop 1; and (iv) not going through either hoops. According to Theorem 1 each path is the least cost one in the graph and in its respective homotopy class.

Figure 6(b) shows the exploration of 4 homotopy classes in and around a room with windows on each wall. The skeletons for this obstacle are defined as loops around each window according to Construction 2. The trivial shortest path from the given start to goal configuration goes outside the room (the dark violet trajectory). Trajectories in other homotopy classes pass through the room.

*2) Environment with unbounded Pipes:* Figure 7(a) shows a more complex environment consisting of 7 pipes stretching to infinity. The workspace of choice is $44 \times 44 \times 44$ discretized, with the start and goal coordinates at two opposite corners of the discretized space. In Figure 7(a) we find the least cost paths in 10 different homotopy classes.

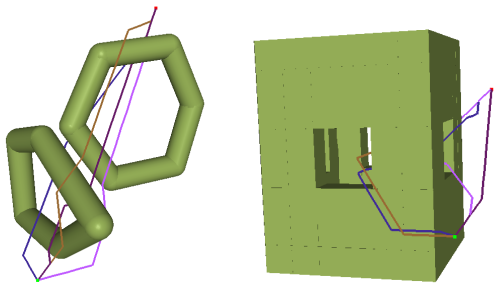

(a) Two hoops. (b) A room with windows.

Fig. 6. Exploring homotopy classes in $X - Y - Z$ space.

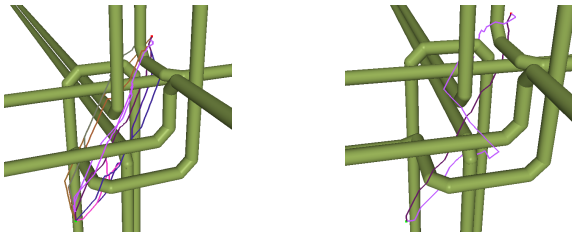

(a) Exploring 10 distinct homotopy classes. (b) Plan in the *complementary homotopy class* of the least cost path.

Fig. 7. An environment with 7 unbounded pipes.

*3) Planning with Homotopy Class Constraint:* Figure 7(b) demonstrates a planning problem with homotopy class constraint. The darker trajectory is the global least cost path found from a search in $\mathcal{G}$ for the given start and goal coordinates. The *h*-signature for that trajectory was computed, and hence we computed the signature of the *complementary homotopy class* (Definition 6), and put it in $\mathcal{A}$. The lighter trajectory is the one planned with that $\mathcal{A}$ as the set of allowed *h*-signature. This trajectory goes on the *opposite side* of each and every pipe in the environment as compared to the darker trajectory.

*4) Search Speed and Efficiency:* We now present the running time for the case in Figure 7(a). The environment, as described earlier, is $44 \times 44 \times 44$ discretized, and hence $\mathcal{G}$ contains $85184$ nodes. Due to each node being connected to $26$ of its neighbors, there are almost $13$ times as many edges in $\mathcal{G}$. The program was run on a Intel Core 2 Duo processor with 2.1 GHz clock-speed and 3GB RAM. We first compute the values of $\mathcal{H}(e)$ for all edges $e \in \mathcal{E}$ and store them in a cache, which takes about $2273s$. Then we perform the A* search in $\mathcal{G}_H$, using the values from the cache whenever required. By doing so we eliminate the requirement of re-computing the *h*-signatures of the edges every time we perform a search, even with changed start and goal coordinates. The search for the $10$ homotopy classes in Figure 7(a) took about $30s$ and expansion of $521692$ nodes in $\mathcal{G}_H$. Figure 8 shows the cumulative time required and the number of nodes in $\mathcal{G}_H$ expanded.

### B. Planning in 2-dimensional plane with moving obstacles

The next 3-dimensional domain that we experiment with is that of the two-dimensional plane, but with dynamic entities. Thus the variables of interest are $X, Y$ and $time$. The node set was formed by uniform discretization of the domain of interest. The connectivity of the graph is such that the *time* variable can increase only in the positive direction (each node connected to 9 neighboring nodes in next time step, including

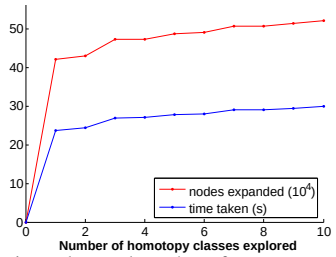


Fig. 8. Cumulative time taken and number of states expanded while searching $\mathcal{G}_H$ for 10 homotopy classes in the problem of Figure 7(a).

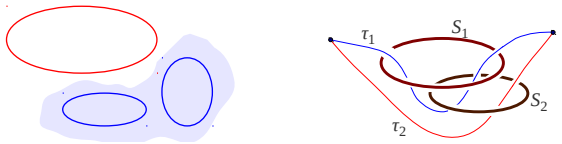


(a) 2 non-homeomorphic manifolds belonging to same homology class. (b) An example where the trajectories are homologous, but not homotopic

Fig. 10. An overview of homology of 1-dimensional manifolds.

the same $x$ & $y$). The cost of an edge, $e$, with differences in the coordinates of its end points $\Delta x, \Delta y$ and $\Delta t$ is computed as $c(e) = \sqrt{\Delta x^2 + \Delta y^2 + \epsilon \Delta t^2}$, where $\epsilon$ is a small value for avoiding *zero cost edges* in $\mathcal{G}_H$. The skeleton of the moving obstacles are the curves traced by their centers (yellow dots in Figure 9) in the $X-Y-Time$ space. The skeletons are closed outside and far from the discretized domain (Construction 1). Note that in doing so, segments of the skeleton may point along negative time. However that does not effect the planning since the $X - Y - Time$ space itself can be treated no differently from $\mathbb{R}^3$.

Figure 9 shows the screen-shots from exploration of $4$ homotopy classes in $X-Y-Time$ domain. The environment is $40 \times 40$ discretized in $X$ and $Y$ directions, and have $100$ discretization cells in time. There are two dynamic rectangular obstacles, $\mathcal{O}_1$ and $\mathcal{O}_2$, that undergo a known oscillatory motion inside a narrow passage between other static obstacles. The $4$ different trajectories in the different homotopy classes are marked by different colors as well as different numbers at their current locations. The trajectories in the non-trivial homotopy classes *go behind* the obstacles, a region that would otherwise not be visited by the least cost path without any homotopy class consideration.

## VI. Homotopy as an Approximation of Homology

As discussed earlier, the Assumption 1 may not always hold true. The reason is, in strictest sense the *h*-signature is a *homology* invariant rather than homotopy invariant. The study of homology theory as a part of algebraic topology emerged in the fist place because homotopy is difficult to deal with computationally [9]. Although there is much similarity between homotopy and homology, the later is more abstract in nature. However homology is computationally favorable. Thus, very often homology is used as a modest substitute of homotopy.

The integrand in Ampere's law that we used in defining the *h*-signatures can be shown to be elements from *De-Raham cohomology* groups [12, 14], which forms a dual to homology groups of 1-dimensional manifolds (robot trajectories in our

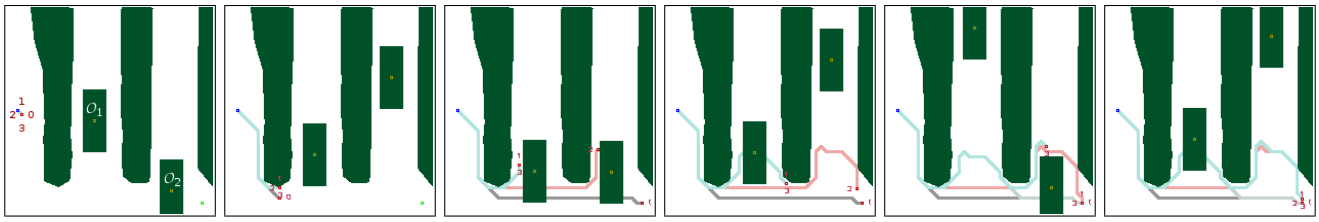


(a) $t = 0.4s$ (b) $t = 8.6s$ (c) $t = 23.7s$ (d) $t = 29.6s$ (e) $t = 37.0s$ (f) $t = 43.1s$

Fig. 9. Screen-shots from an example with two moving obstacles ($\mathcal{O}_1$ and $\mathcal{O}_2$) showing the exploration of 4 homotopy classes in a dynamic environment. The blue trajectory (3) passes above both $\mathcal{O}_1$ and $\mathcal{O}_2$. The red trajectory (2) passes above $\mathcal{O}_2$, but not $\mathcal{O}_1$. The light blue-gray trajectory (1) passes above $\mathcal{O}_1$, but not $\mathcal{O}_2$. The dark gray trajectory (0) is the trivial shortest path.

case). Thus the *h*-signatures can be shown to be homology invariants of the trajectories[2].

Without going into in-depth discussions on homology theory, we would like to emphasize a few important similarities between homology and homotopy, especially in relation to the application discussed in this paper:

i. Two manifolds are homotopic implies that they are homologous [9, 14]. Thus, two trajectories that are homotopic will be in the same homology class as well, and hence their *h*-signatures will be the same. Thus, in the problems where we find least cost trajectories in different homotopy classes in a configuration space using the proposed algorithm, we are always guaranteed to obtain the trajectories in distinct homotopy classes in spite of using the *h*-signature.

ii. For two 1-dimensional manifolds to be homologous, they need not be homeomorphic in general (*e.g.* one can have 2 connected components, while the other can have 1 as shown in Figure 10(a)). However, since robot trajectories are always homeomorphic to $[0, 1]$, the separation between homology and homotopy for robot trajectories is even less.

iii. The inverse of statement i. (*i.e.* homologous implies homotopic) for robot trajectories holds true for lots of practical robotics problems. For example, it holds true without exception when the obstacles extend to infinity (or to outside the domain of interest) in both directions without forming knots. Thus, for example, in problems with dynamic 2-D obstacles (Sec. V-B), homotopy and homology are one and same.

We conclude with an example where homology is not same as homotopy. In Fig. 10(b), one can observe that the two trajectories are not homotopic in the total space of the obstacles, but they are homotopic with respect to individual obstacles. Hence their *h*-signatures are the same (*i.e.* they are homologous). Thus, if we were exploring different homotopy classes in this environment using the described method, we would be finding one trajectory for these two homotopy classes.

## VII. Conclusion

In this paper we have proposed a novel and efficient way of representing homotopy classes in 3-dimensional configuration spaces by exploiting laws from theory of electromagnetism. We have shown that this representation is well suited for use with graph search techniques for finding least cost paths respecting given homotopy class constraints as well as for exploring different homotopy classes in an environment. The method is independent of the discretization scheme or the cost function. We have demonstrated the efficiency, applicability and versatility of the method in our results. Although, in strict mathematical sense the equivalence relation under consideration is *homology*, we argued that it equates to homotopy in most practical robotic applications.

[2]In strict sense, homology classes can be defined only for closed (boundaryless) curves. Here, by two trajectories being homologous we mean that the closed loop formed by them is *null-homologous*.

## References


[1] Subhrajit Bhattacharya, Vijay Kumar, and Maxim Likhachev. Search-based path planning with homotopy class constraints. In *Proceedings of the Twenty-Fourth AAAI Conference on Artificial Intelligence*, Atlanta, Georgia, July 11 2010.

[2] Subhrajit Bhattacharya, Maxim Likhachev, and Vijay Kumar. *h*-signature of a non-looping trajectory with respect to an infinite straight line skeleton. Technical report, The University of Pennsylvania, May 2011. See https://fling.seas.upenn.edu/∼subhrabh/cgi-bin/wiki/index.php?SFile=RSS11supp.

[3] Harry Blum. A Transformation for Extracting New Descriptors of Shape. In Weiant W. Dunn, editor, *Models for the Perception of Speech and Visual Form*, pages 362–380. MIT Press, Cambridge, 1967.

[4] Frederic Bourgault, Alexei A. Makarenko, Stefan B. Williams, Ben Grocholsky, and Hugh F. Durrant-Whyte. Information based adaptive robotic exploration. In *in Proceedings IEEE/RSJ International Conference on Intelligent Robots and Systems (IROS*, pages 540–545, 2002.

[5] Douglas Demyen and Michael Buro. Efficient triangulation-based pathfinding. In *AAAI'06: Proceedings of the 21st national conference on Artificial intelligence*, pages 942–947. AAAI Press, 2006.

[6] David J. Griffiths. *Introduction to Electrodynamics (3rd Edition)*. Benjamin Cummings, 1998.

[7] D. Grigoriev and A. Slissenko. Polytime algorithm for the shortest path in a homotopy class amidst semi-algebraic obstacles in the plane. In *ISSAC '98: Proceedings of the 1998 international symposium on Symbolic and algebraic computation*, pages 17–24, New York, NY, USA, 1998. ACM.

[8] P. E. Hart, N. J. Nilsson, and B. Raphael. A formal basis for the heuristic determination of minimum cost paths. *IEEE Transactions on Systems, Science, and Cybernetics*, SSC-4(2):100–107, 1968.

[9] Allen Hatcher. *Algebraic Topology*. Cambridge University Press, 2001.

[10] John Hershberger and Jack Snoeyink. Computing minimum length paths of a given homotopy class. *Comput. Geom. Theory Appl*, 4:331–342, 1991.

[11] Anil K. Jain. *Fundamentals of digital image processing*. Prentice-Hall, Inc., Upper Saddle River, NJ, USA, 1989.

[12] J. Jost. *Riemannian Geometry and Geometric Analysis*. Springer, 2008.

[13] James Munkres. *Topology*. Prentice Hall, 1999.

[14] Joseph J. Rotman. *An Introduction to Algebraic Topology*. Springer, 1988.

[15] E. Schmitzberger, J.L. Bouchet, M. Dufaut, D. Wolf, and R. Husson. Capture of homotopy classes with probabilistic road map. In *International Conference on Intelligent Robots and Systems*, volume 3, pages 2317–2322, 2002.

[16] Yves Talpaert. *Differential Geometry with Applications to Mechanics and Physics*. CRC Press, 2000.

[17] Yan Zhou, Bo Hu, and Jianqiu Zhang. Occlusion detection and tracking method based on bayesian decision theory. In Long-Wen Chang and Wen-Nung Lie, editors, *Advances in Image and Video Technology*, volume 4319 of *Lecture Notes in Computer Science*, pages 474–482. Springer Berlin / Heidelberg, 2006.